ARTICLE IN PRESS

Available online at www.sciencedirect.com

SCIENCE DIRECT®

ELSEVIER

Sensors and Actuators B 6954 (2003) 1–9

SENSORS AND ACTUATORS B CHEMICAL

www.elsevier.com/locate/sensorb

Performance of the Spreeta 2000 integrated surface plasmon resonance affinity sensor

T.M. Chinowsky[a,*], J.G. Quinn[b], D.U. Bartholomew[b], R. Kaiser[c], J.L. Elkind[b]

[a]*Department of Electrical Engineering, University of Washington, P.O. Box 352500, Seattle, WA 98195-2500, USA*
[b]*Texas Instruments Inc., 13536 N. Central Expressway, Dallas, TX 75243, USA*
[c]*Prolinx Inc., 22322 20th Avenue SE, Bothell, WA 98021, USA*

Abstract

Surface plasmon resonance (SPR) has become well established as a laboratory tool for the study of biological binding reactions, but has had limited application outside of this context. With the goal of moving SPR applications from high-cost systems designed for central laboratories to low-cost, portable electronic systems designed for the field, Texas Instruments Inc. (TI), has developed Spreeta, a line of compact, integrated SPR sensor components. This paper reports on the performance of TI's newest SPR device, the Spreeta 2000, measured using instruments developed by TI and by Prolinx Inc., who are developing advanced molecular interaction analysis technology utilizing a proprietary version of Spreeta 2000.

Noise optimization techniques including averaging and sum normalization are discussed, and the dependence of refractive index (RI) noise on these techniques is measured. For a measurement time of 0.8 s, a noise level of 1.8×10^{-7} RI is observed. To estimate the accuracy potentially obtainable using the sensor, the smoothness of the sensor response is measured using RI gradients, and is found to be 0.2% over a change in RI of 0.04.

As a demonstration of the capabilities of the Spreeta 2000 when incorporated into an appropriate instrumentation system, an automated assay for mouse IgG is presented.

Keywords: Surface plasmon resonance; Biosensor; Spreeta; Refractive index

1. Introduction

Surface plasmon resonance (SPR) affinity sensors detect chemical or biological substances by measuring their binding to the sensor surface [1]. This binding is measured by monitoring changes in the refractive index (RI) close to the sensor surface; any binding or adsorption process creating a change in surface RI may be measured. When combined with appropriate biochemical surface functionalization, SPR provides a powerful and versatile tool for detecting and characterizing biomolecular interactions.

1.1. Spreeta, the Texas Instruments Inc. (TI) SPR sensor

SPR has become well established as a laboratory tool for the study of biological binding reactions, but has had limit application outside of this context. With the goal of moving SPR applications from high-cost systems designed for central laboratories to low-cost, portable electronic systems designed for the field, TI has developed Spreeta, a line of compact, integrated SPR sensor components designed to be manufacturable in very large quantities [2–6]. The Spreeta devices contain all of the optical components necessary to implement SPR sensing, yet are low-cost enough to be compatible with disposable applications. Spreeta technology has major potential benefits for fields including medical diagnostics, environmental monitoring, and food and water safety. Spreeta technology enables inexpensive, quantitative, electronic point-of-care (POC) biosensing instrumentation for use in the hospital, physician's office, emergency transport, or anywhere POC testing is needed. For environmental monitoring, Spreeta instrumentation can be sufficiently lightweight and low power to be battery operated and used in the field to check for soil or water contamination. For food and water safety applications, disposable Spreeta sensors enable for real-time process control, for instance to monitor antibiotic content in meat and dairy production.

* Corresponding author. Tel.: +1-206-616-5558; fax: +1-206-543-3842.
E-mail address: timc@u.washington.edu (T.M. Chinowsky).

0925-4005/03/$ – see front matter © 2003 Published by Elsevier Science B.V.
doi:10.1016/S0925-4005(03)00113-8

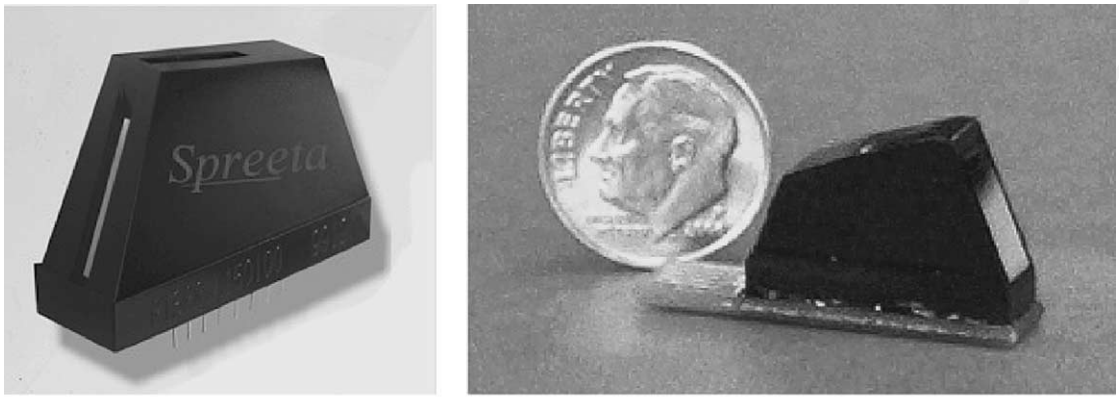

(a) (b)

Fig. 1. Photograph of Spreeta components. (a) Original Spreeta, (b) Spreeta 2000.

The first mass-produced Spreeta device, introduced in 1999, measures approximately 3 cm × 1.5 cm × 4 cm and provides electrical connections using a 16-pin DIP connector (Fig. 1a). In 2001, TI began production of the newest Spreeta device, the Spreeta 2000 (S2K). This device is smaller than the original Spreeta (1.5 cm × 0.7 cm × 3 cm) and interfaces using a miniature 10-pin card-edge connector (Fig. 1b). In this paper, we will describe the Spreeta 2000 sensor, characterize two aspects of its performance (noise and response smoothness) and present an example of a biosensing application which illustrates the use of the device.

1.2. Spreeta sensing principle

The Spreeta sensor consists of a plastic prism molded to a microelectronic circuit contained on a printed circuit board (PCB) (Fig. 2). The circuit contains an infrared LED (830 nm peak wavelength), a 128-pixel linear diode array detector, and a non-volatile memory chip for recording identification and calibration information. The LED emits a diverging beam that passes through a polarizer and strikes an elliptical region of the sensor surface at a range of angles above the critical angle. The angle at which light is incident upon this surface will vary with the location on the surface: smaller incident angles strike closer to the base of the sensor.

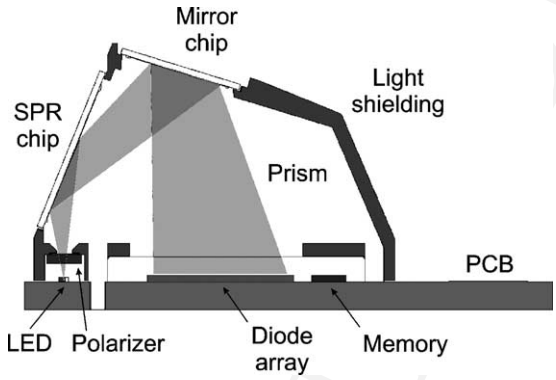

Fig. 2. Cross section of the Spreeta 2000, showing components of the sensor and the path followed by light inside the sensor.

The sensor surface is formed by a glass chip coated with a ~50 nm layer of gold and epoxied to the plastic prism. The thin layer of gold produces the SPR effect: for certain angles of incidence, part of the energy of the transverse-magnetic (TM) polarized incident light will couple into a surface plasma wave traveling along the interface between the gold layer and the analyte. The loss of this energy is observed as a sharp attenuation of reflectivity. The angles at which this occurs vary with the surface RI of the analyte; therefore one can measure the surface RI by measuring the reflectivity across a range of angles and analyzing the resulting reflection spectrum. In the Spreeta, the light reflected from the sensor surface then reflects from the sensor's top mirror and back down onto the PCB. A portion of this light strikes the diode array detector. Because each detector pixel will collect light which struck the sensor surface at a different angle, a reflectivity versus angle spectrum may be obtained by reading the detector array. The active area on the sensor surface (i.e. the area on which the RI is sensed) is defined by the portion of the light cone which projects onto the detector, and is a strip 0.2 wide by 3 mm long.

1.3. The Prolinx Octave instrument

Prolinx Inc. (Bothell, WA) [7] are using Spreeta 2000 technology to develop the Prolinx Octave Molecular Interaction Analysis System, which combines a proprietary version of the Spreeta 2000 with Prolinx Versalinx chemistry in a compact, high-performance instrument for rapid and efficient biomolecular interaction analyses. Versalinx chemistry is based upon the interaction of phenyl(di)boronic acid (P(D)BA) and salicylhydroxamic acid (SHA) to form a complex. SHA and P(D)BA are a synthetic, small molecule, low molecular weight affinity pair that can be used for the facile immobilization of nucleic acids, proteins and other macromolecules. SHA substrates, such as the monolayer on the Octave sensor chip, are universal in that they will bind any P(D)BA labeled macromolecule.

The Octave incorporates eight independent S2K sensors operating in parallel. The sensors are arrayed on 9 mm centers,

producing a sensor format highly compatible with manipulation of samples held in industry standard 96-well plates.

The instrument incorporates A/D and D/A converters, programmable logic and a powerful digital signal processor (DSP) to provide LED drive current, generate photodiode array timing signals, digitize sensor outputs to high resolution, and perform many of the calculations necessary for analysis of the SPR signals. The Octave instrument interfaces to a personal computer (PC) over a universal serial bus (USB) interface. PC-based custom software provides an easy to use graphical user interface for manipulating instrument functions, performing automated experiments, and storing and analyzing sensor data.

The data presented in this paper was generated using both a prototype Octave instrument and simpler hardware distributed by TI for evaluation of the S2K. The Octave hardware is designed to extract optimal performance from the S2K sensors, and was used for the characterization of Spreeta noise presented below. Data from evaluation hardware was used to collect the other data; the noise level of this data is higher than the Octave data, but is representative of Spreeta performance in other respects.

2. Spreeta 2000 manufacturing process

The construction of the S2K is compatible with very high-volume production. The sensor has four main components—the injection-molded "sail" containing the plastic prism, polarizer, and light shielding; the printed circuit board containing the sensor's electronic components; and the glass mirror and SPR sensing chips. The process steps involved in construction of the S2K are listed in Table 1.

Table 1
Manufacturing steps for production of Spreeta 2000

1	Wire bond LED, photodiode array, memory chip to sensor PCB
2	Test LED, photodiode array, memory for functionality
3	Injection-mold clear polycarbonate sensor prism
4	Inject black polycarbonate to form light shielding surrounding prism
5	Attach polarizer to sail using epoxy
6	Attach sail to PCB, using pins on sail and clear epoxy
7	Add black epoxy to complete light shielding
8	Attach mirror to upper prism surface using epoxy
9	Attach SPR chip to sensor surface using epoxy
10	Test LED, photodiode array, memory for functionality
11	Measure sensor spectra in air and water

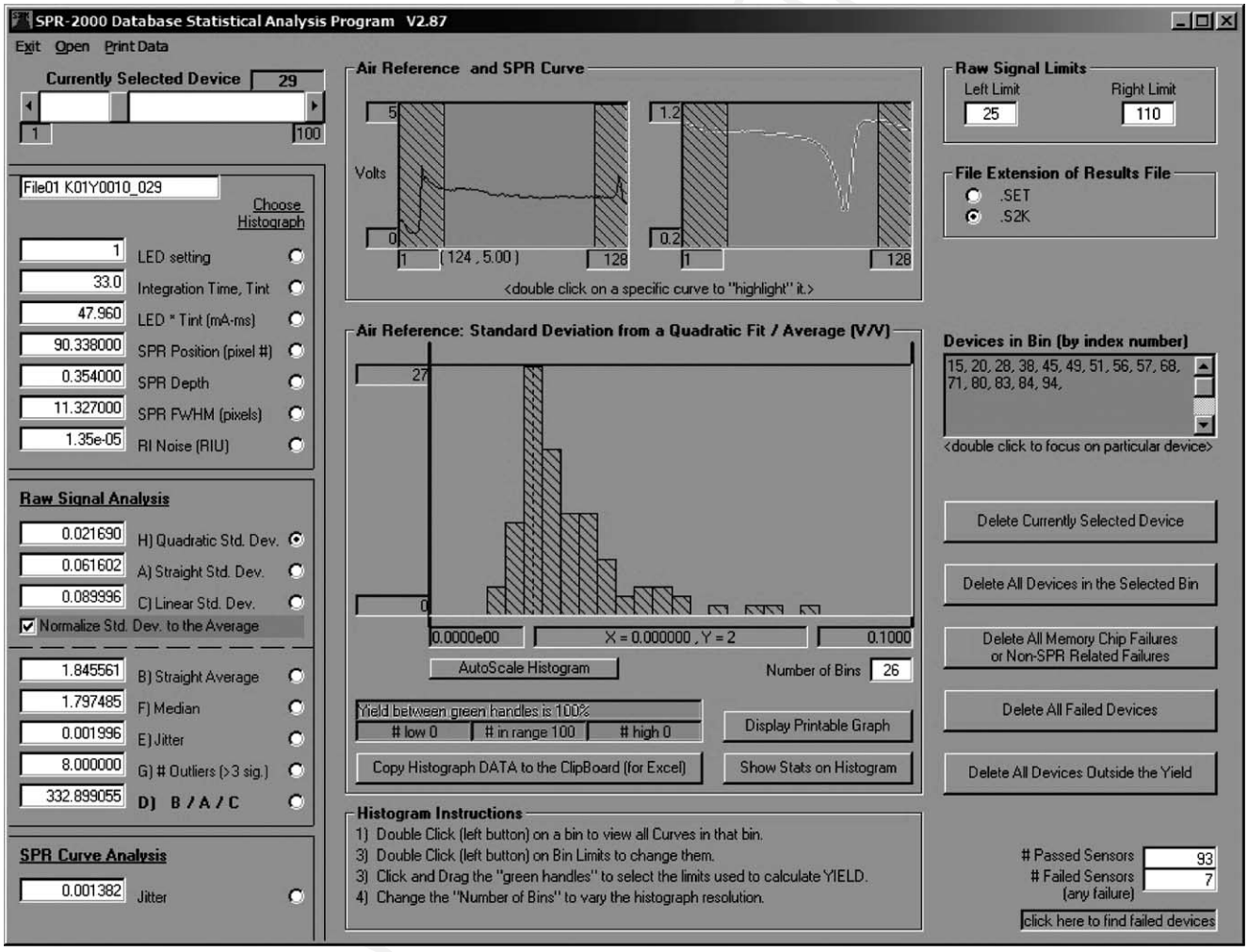

Fig. 3. Screen capture from TI's Spreeta 2000 statistical analysis software.

As with any manufacturing process, the yield of the Spreeta manufacturing process and the uniformity of the sensors is of prime concern. TI tests each sensor both for electronic functionality (correct functioning of LED, detector, and memory) and for optical performance, measuring SPR spectra in air and in water. Critical sensor parameters, including the location, depth, and width of the sensor's SPR curve, and the smoothness of the sensor's raw signal output, are calculated and recorded. The data for each lot of sensors are compiled using custom software developed by TI (Fig. 3), in which parameter statistics are easily manipulated and associated with the specific sensor data contributing to that statistic. The overall process yield is greater than 90%.

3. Spreeta 2000 performance characteristics

3.1. Sensor noise

Two sensor characteristics which have particular significance for biosensing applications are noise level and accuracy. The noise level present in the RI measurements performed by an SPR sensor places a lower bound on the amount of bound material that can be detected. For example, a RI change of 10^{-6} corresponds to a surface coverage of $\sim$1 pg/mm^2 of protein on a 2-D surface [8].

Three factors which contribute to the noise observed in the Spreeta are detector noise, shot noise, and LED fluctuations. Detector noise represents the intrinsic noise present on the output of the sensor's photodiode array due to electronic processes within the detector. Shot noise is caused by the statistical fluctuation in the quantity of light which reaches each detector pixel in an integration period. Noise due to LED fluctuations results from variations in light source intensity due either to intrinsic properties of the LED or to external factors such as fluctuations of LED drive current or temperature variations.

The first step in optimizing the noise performance of a device is to choose components with intrinsically low noise. Once further reduction in intrinsic light source and detector noise is no longer possible due to technological or cost limitations, the optimal way of operating the sensor to minimize the effect of the remaining noise sources must be determined. The different properties of each type of noise leads to different manifestations in the data and require different strategies for reducing or eliminating noise effects. For the Spreeta, the light source intensity and detector integration time must be optimized. Noise level is not the only factor to consider in this optimization—for instance, if very rapid measurements are needed, noise reduction due to signal averaging may be sacrificed in exchange for an increase in measurement speed. If it is important to minimize power dissipation in the sensor, a decrease in LED drive level may be desirable even though noise level may increase.

The way in which data is processed (averaging, extraction of RI from SPR curves) must also be optimized for best noise performance. Two important techniques for noise reduction—spectral averaging and sum normalization—and their effects on sensor noise are described below.

3.1.1. Effect of spectral averaging on observed RI noise

The intrinsic noise level produced by the S2K's diode array detector is on the order of 0.1% of full-scale response. The first and most important technique available for reducing the effects of this noise is spectral averaging—i.e. rather than extracting an RI measurement from one measured spectrum, a number of spectra are first averaged together, and the RI measurement extracted from the average. When the S2K is operated with short integration times and with high-performance hardware such as that in the Octave instrument, high levels of averaging and a substantial reduction of noise are possible.

Fig. 4 shows the RI noise level observed during S2K measurements of distilled water using the Octave instrument, for various degrees of averaging. LED current and detector integration time were chosen for best noise performance, and were $I_{LED} = 20$ mA, and $T_{INT} = 5$ ms. The RI was measured repeatedly for 2–4 min. The measurements were detrended using a quadratic polynomial to remove the effects of sensor drift, and the standard deviation of the residual was calculated. This value was then plotted as a function of the time required to acquire the measurement, as estimated by multiplying the integration time by the number of spectra averaged together. (Note that the actual measurement time will be slightly greater than the plotted time, due to the additional time required to digitize the detector output. For the Octave operating at 5 ms integration time, this adds about 10% to the measurement acquisition time.)

It is observed that straightforward averaging of spectra (points marked with dots on Fig. 4), while effective in

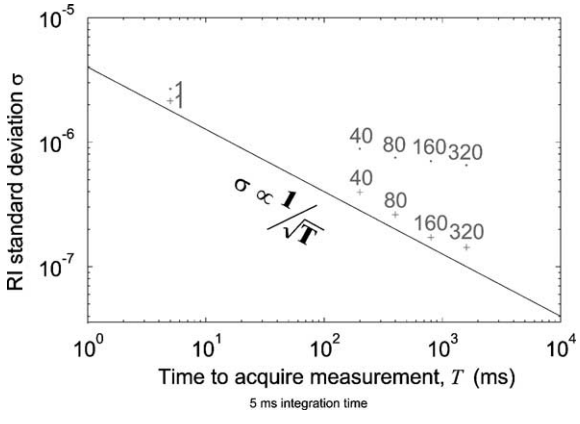

Fig. 4. Noise level of RI measurements of water measured using Spreeta 2000 in the Prolinx Octave instrument, as a function of measurement time. Numbers indicate the number of SPR spectra averaged together to obtain each measurement. Points marked with "·" were calculated using raw spectra; points marked with "+" were calculated using sum-normalized spectra (see text for details).

reducing sensor noise level, is not as effective as would be expected if the noise behaved like uncorrelated white noise: For an average of N spectra, a noise level proportional to 1/sqrt(N) would be expected, and the observed reduction is rather less effective. This is consistent with the presence of noise with a non-white spectral characteristic such as 1/f noise [9] which cannot be reduced through averaging. The nature of this noise component becomes clear when the pixel-to-pixel correlation of the noise is examined. In raw (un-averaged) spectra, there is little pixel-to-pixel correlation of the observed noise, as would be expected for intrinsic detector or shot noise. In highly averaged spectra, a pronounced correlation of noise across all pixels is observed, suggesting that the uncorrelated white noise component has been largely eliminated through averaging, revealing an underlying noise component affecting all pixels and possessing a 1/f characteristic. Likely sources of this correlated noise include LED intensity variations due to variations in LED drive current, intrinsic LED flicker noise, and temperature fluctuations; temperature-induced variations in detector sensitivity would have similar effects.

3.1.2. Reduction of correlated noise using sum normalization

Optical instrumentation is often designed to compensate for noise contributions of light source variations—the light level is continuously measured, and measurements compensated for light level during data analysis. The same technique can be applied to Spreeta 2000 data using a simple sum normalization technique, in which the sum of the pixels in part or all of the measured spectrum is used as to provide a measurement of light level. Each pixel's value y_i, $i = 1, \ldots, 128$ will be the product of light intensity I and the reflectivity at the sensor surface for that pixel, R_i, which is a function of the surface RI, n:

$$y_i(t) = I(t)R_i(n) \quad (1)$$

If R_i were constant, each pixel value would be proportional to I and could be used as a measurement of light intensity. However, because the detector noise on each pixel taken separately is substantial, and because R_i will in general change with n, this is impractical. However, a *sum* of detector pixels, for instance of pixels $i_1 < i < i_2$, will have reduced noise due to averaging, and can be used to provide a measurement proportional to light intensity:

$$\sum_{i=i_1}^{i_2} y_i(t) = I(t)\sum_{i=i_1}^{i_2} R_i(n) \cong cI(t) \quad (2)$$

However, Eq. (2) holds only if that the sum of reflectivities is fairly constant. This may be achieved by taking the sum over a range of pixels outside the range where the reflectivity is affected by SPR. However, we have found that even if the sum is taken over all 128 pixels of the detector, the sum will typically remain constant to within 1%—as the SPR dip moves from pixel to pixel during the experiment, individual pixel values change, but the sum of all pixels remains relatively constant.

This simple method of sum normalization results in a significant reduction in RI noise (Fig. 4). The noise level of the normalized data conforms more closely to the 1/sqrt(N) averaging characteristic expected of white noise, and a covariance matrix analysis of the normalized spectra indicates little pixel-to-pixel noise correlation in the normalized spectra, suggesting that the normalization has successfully removed the bulk of correlated and non-white noise. In the sum-normalized data, a noise standard deviation of 3.7×10^{-7} RI units is observed for a measurement time of 0.2 s (40 averages); for a measurement time of 0.8 s (160 averages) noise decreases to 1.8×10^{-7} RIU.

3.2. Smoothness of sensor response

A second important sensor characteristic is accuracy. The accuracy of the Spreeta 2000 RI measurements (in combination with the reproducibility of the sensor chemistry) will determine the degree to which the sensor can be used for quantitative measurements, and also determines the extent to which the SPR measurements from two different experiments or sensors can be compared, for instance for compensation of non-specific binding, bulk RI, or temperature effects. Because the Spreeta 2000, like any SPR sensor, requires calibration to produce accurate RI measurements, the accuracy expected from the sensor is a function of how easy it is to calibrate the sensor. This in turn is a function of the smoothness of the sensor response—if the sensor's natural response is smooth, it can generally be calibrated using a simple functions (e.g. low order polynomials), the coefficients of which may be determined by a small, easily performed set of measurements. For this reason, we use the smoothness of the sensor's response over a given operating range as a measure of the accuracy obtainable from the sensor under optimal conditions.

A simple and sensitive method for examining sensor smoothness is through the use of RI gradients: the sensor is exposed to a solution which slowly and smoothly varies in RI over the range of interest [10], and the sensor response is measured throughout the gradient. One simple setup for producing RI gradients is shown in Fig. 5.

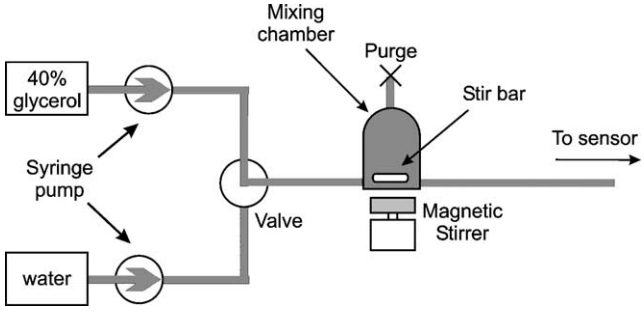

Fig. 5. Schematic of apparatus used for producing exponential RI gradients for characterization of sensor smoothness.

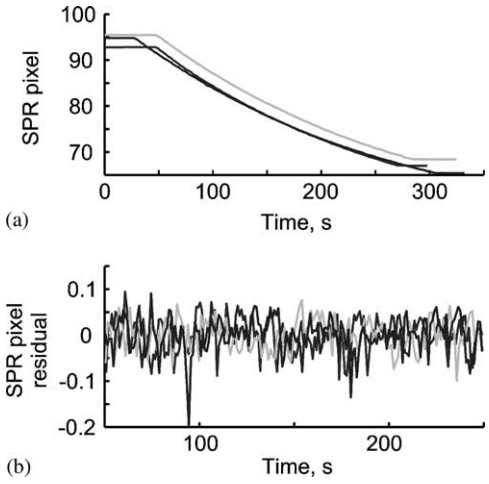

Fig. 6. Characterization of smoothness of response of three Spreeta 2000 sensors. (a) Variation of SPR pixel position during exposure to exponential RI gradient ranging over $\Delta n = 0.04$. (b) Data from (a), detrended using a fourth order polynomial. Standard deviation of residual is ~0.2% of range.

A dual syringe pump containing water and 40% glycerol is connected to a two-port injector valve. The valve output leads to a stirred mixing chamber (volume V, ~1.4 ml). Because the mixing chamber is completely filled with liquid and sealed except for its two fluid connections, the glycerol concentration of the solution leaving the mixing chamber (and, by assumption, the concentration of the solution inside the chamber) is described by the equation:

$$\frac{dc_{out}}{dt} = \frac{q_p}{V}(c_{in} - c_{out}) \quad (3)$$

where q_p is the flow rate of the syringe pump. If a particular output concentration profile is desired, this equation must be solved to determine how c_{in} must vary to produce that profile. In the data presented here, the mixing chamber was initially filled with water, and the input solution was simply switched between water and 40% glycerol at the beginning of the experiment. This results in an approximately exponential RI profile extending from $n = 1.33$ to 1.37. The raw data resulting from exponential gradients run on three different S2K sensors is shown in Fig. 6a. To quantify the curve roughness, a fourth order polynomial was fit to the these plots and the residuals calculated (Fig. 6b). The standard deviation of the residual was 0.03–0.04 pixels, or 0.2% of the RI range of the experiment.

Of course, this performance does not guarantee assay accuracy at the 0.2% level—to evaluate assay accuracy, many other experimental factors such as reproducibility of assay chemistry must taken into account. Rather, we take this figure as an estimate of the accuracy obtainable by the S2K sensor component by itself, and interpret it to mean that the component itself will not be a limiting factor in assay accuracy down to below the 1% level.

4. Sample application: assay for the detection of mouse IgG

The interaction of protein A, a bacterial cell wall protein, with the Fc region of many immunoglobulin G (IgG) antibodies is routinely exploited for the purification of IgG by affinity chromatography. The protein A–mouse IgG interaction is characterized by high-binding affinity and excellent regeneration capability: bound antibody may be released almost completely by exposing the protein A–IgG complex to low pH (i.e. pH 2.0). Despite repeated exposure to low pH the binding capacity of the protein A coated surface is stable for several hundred binding–regeneration cycles.

Here we use this protein–protein interaction to demonstrate the ability of Spreeta 2000 to obtain quantitative data describing such interactions. The quantitation of antibodies

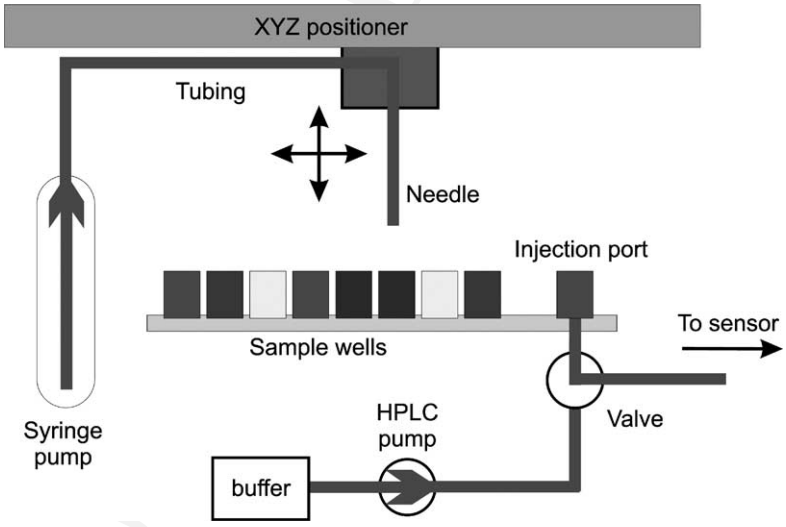

Fig. 7. Schematic of autosampler setup used to perform an automated IgG assay with Spreeta 2000. See text for details.

contained in hybridoma supernatants, serum, or other sample matrices is of broad interest and is typically accomplished by enzyme-linked immunosorbent assay (ELISA). This technique is inexpensive but is time consuming. Spreeta technology provides a rapid, inexpensive and versatile alternative. Similar to affinity chromatography, the protein A is immobilized onto the solid phase while the sample, containing the antibody, is exposed to this sensing surface. Labeling of reagents is not required, as the SPR transducer enables direct monitoring of biomolecular binding by observing RI changes at the sensing surface. In addition, the real-time interaction data enables direct feedback and considerable assay design flexibility.

4.1. Apparatus

An automated instrument using the Spreeta 2000 was constructed (Fig. 7). An injection needle was attached to 3 ft of 1/16 in. tubing and fitted to a 0.5 ml Hamilton syringe. The syringe was fitted to a syringe pump and the needle was mounted on a robotic arm. Samples were placed in an aluminum sample block that was cooled to prevent sample evaporation and to preserve the biological activity of the samples. A flow cell (volume 100 nl) was constructed and clamped to the sensor surface. A two-way computer-controlled valve leading to the Spreeta flow cell was configured to switch between an injection port and an HPLC pump, as follows: while the electronic valve is switched to position "A", constant running buffer from the HPLC pump is switched through the Spreeta flow cell. In position "B" the injection port is connected to the flow cell, while the running buffer is directed to waste. To inject a sample or regeneration solution through the flow cell, the sample is aspirated by the autosampler and injected into the injection port; after a slight delay the valve switches from "A" to "B", sending the injection to the flow cell. Once the injection is completed, the valve is switched back to "A" to resume the flow of constant flow buffer through the flow cell.

The volume between the injection port and the flow cell was minimized (to less than 1 μl) to minimize dispersion effects. HPLC fittings are used at all junctions to minimize dead volumes. Custom control software was written to control the sample handling robot, pumps, valve, and data collection, allowing unattended analysis of samples.

4.2. Assay procedure and results

A Spreeta 2000 sensor surface was coated with a hydrogel and then functionalized with protein A. A mass of protein A equivalent to 800 μRIU was immobilized onto the surface using conventional EDC/NHS coupling. Serial doubling dilutions of mouse IgG were prepared in running buffer from 25,000–1.5 ng/ml (i.e. 160,000–10 pM approximately). All buffers were degassed and filtered before use, and were allowed to equilibrate to room temperature for several hours to reduce temperature related drift. The sensor was turned on and allowed to warm up for 20 min.

Each sample was then injected for 2 min at 50 μl/min. A few minutes after each injection, the surface was regenerated with a 1 min pulse of 15 mM HCl. Fig. 8 shows overlaid binding interaction including regeneration.

The sensor's response to various concentrations of IgG is summarized in the titration curve of Fig. 9. To produce this curve, the response due to antibody binding is calculated as the difference in response before and after injection of the antibody sample. This difference is then plotted against the antibody concentration. Fig. 9 shows that the measuring range extends from 160,000 to 80 pM approximately, when fitted with a sigmoidal 4-parameter logistic expression. This range and the limit of detection (∼80 pM) is comparable with that expected from ELISA.

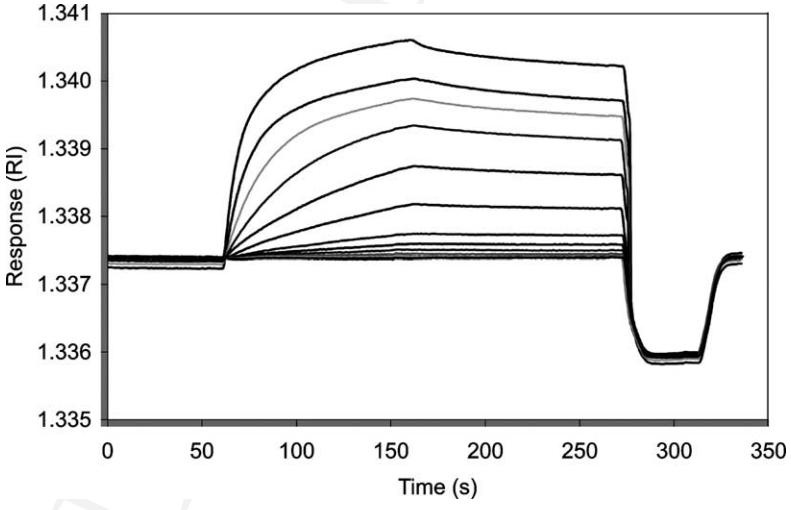

Fig. 8. Overlaid binding interaction plots for IgG antibody concentrations from 25,000 to 1.5 nM interacting with immobilized protein A in a direct assay format.

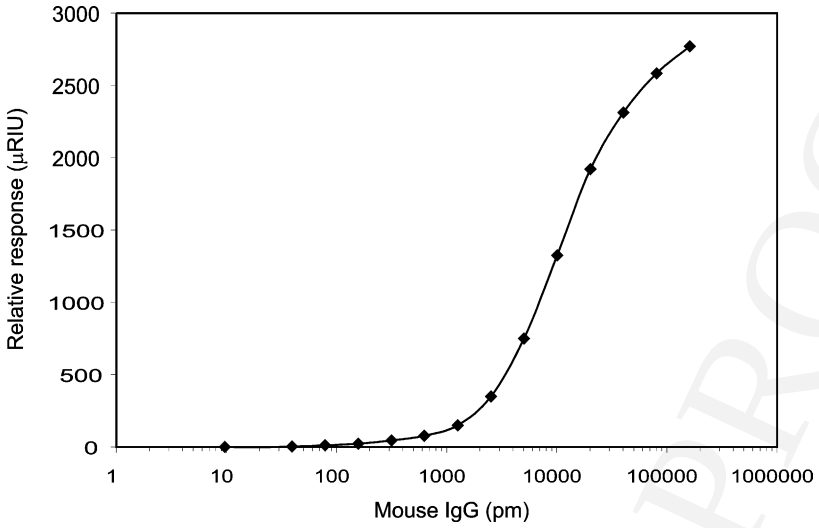

Fig. 9. Titration curve for the detection of mouse IgG using Spreeta 2000 and immobilized Protein A.

Two additional tests were performed to verify other aspects of assay performance. (1) Non-specific binding of a 1 mg/ml solution of BSA in PBS, pH 7.4, was <10 μRIU. (2) As a negative control, free protein A was added, to a final concentration of 25 μg/ml, to an antibody sample containing 25 μg/ml of mouse IgG. The free protein A competitively inhibits binding of the mouse antibody to the immobilized protein A. A binding response of <10 μRIU was observed thus confirming assay specificity and further establishing that non-specific binding was minimal (i.e. ∼0.3% of maximum response).

Note that the baselines of the binding experiments of Fig. 8 have not been aligned during data analysis. The relative offset of the baseline at the beginning of each experiment is that recorded by the instrument at the time, and is caused by a small amount of incomplete regeneration together with instrumental drift over the duration of the experiments. Such drift is commonly removed during post-processing of SPR data; we have retained the drift to illustrate the (quite small) drift observed during the ∼90 min duration of the experiments.

5. Conclusions

Texas Instruments' newest integrated SPR sensor device, Spreeta 2000, incorporates all of the optical and optoelectronic components necessary for implementing SPR biosensing into an inexpensive molded plastic package the size of a thumbnail. When incorporated into a well-designed sensor system, the performance of Spreeta 2000 is sufficient for virtually any SPR biosensing application. The low noise ($\sim 1.8 \times 10^{-7}$ RIU in 0.8 s) and smoothness of response (∼0.2% over $\Delta n = 0.04$) of the sensor, combined with its low-cost, make possible many new distributed SPR sensing applications requiring both high performance and a disposable sensing element.

Acknowledgements

The work described in this paper is the result of the contributions of many people, including the following: from Prolinx, Karin Hughes, Leslie Linkkila, Chris Pershing, Mark Stolowitz, Chris Whalen, and Jean Wiley; from TI, Rick Carr and Pat Smith. For Prolinx Octave hardware and software development, we acknowledge Steve Bailey, Michael Baum, Erik Engstrom, Bob McRuer, and Craig Yamamoto of Stratos Product Development, LLC (Seattle, WA), and Lynn Hilt, Charles Hutchings, Arturo Kozel, George de la Torre, and Terry Weeks of the Ashvins Group (Miami, FL), respectively. In addition, T. Chinowsky acknowledges the support of Texas Instruments, Prolinx, and Sinclair Yee of the Department of Electrical Engineering, University of Washington.

References

[1] S.S. Yee (Ed.), Surface Plasmon Resonance (SPR) Optical Sensors, Current Technology and Applications, Sens. Actuators, B 54 (1999) 1–196.
[2] www.ti.com/spreeta.
[3] J. Melendez, R. Carr, D.U. Bartholomew, K. Kukanskis, J. Elkind, S. Yee, C. Furlong, R. Woodbury, A commercial solution for surface plasmon sensing, Sens. Actuators, B 35 (1996) 1–5.
[4] J. Melendez, R. Carr, D.U. Bartholomew, H. Taneja, S. Yee, C. Jung, C. Furlong, Development of a surface plasmon resonance sensor for commercial applications, Sens. Actuators, B 38–39 (1997) 375–379.
[5] J.L. Elkind, D.I. Stimpson, A.A. Strong, D.U. Bartholomew, J.L. Melendez, Integrated analytical sensors: the use of the TISPR-1 as a biosensor, Sens. Actuators, B 54 (1999) 182–190.
[6] A.A. Strong, D.I. Stimpson, D.U. Bartholmew, T.F. Jenkins, J.L. Elkind, Detection of trinitrotoluene (TNT) extracted from soil using a surface plasmon resonance (SPR)-based sensor platform, Proc. SPIE 3710 (1999) 362–372.

[7] www.prolinx.com.
[8] L.S. Jung, C.T. Campbell, T.M. Chinowsky, M.N. Mar, S.S. Yee, Quantitative interpretation of the response of surface plasmon resonance sensors to adsorbed films, Langmuir 14 (1998) 5636–5648.
[9] C.D. Motchenbatcher, J.A. Connelly, Low-Noise Electronic System Design, Wiley, New York, 1993.
[10] T.M. Chinowsky, S.S. Yee, Data analysis and calibration for a bulk-refractive-index-compensated surface plasmon resonance affinity sensor, Proc. SPIE 4578 (2001) 442–453.